The scaling behavior and mechanism of Ti₂AlC MAX phase coatings in air and pure water vapor

Zongjian Feng [a], Peiling Ke [a,*], Qing Huang [b], Aiying Wang [a,*]

[a] Key Laboratory of Marine Materials and Related Technologies, Zhejiang Key Laboratory of Marine Materials and Protective Technologies, Ningbo Institute of Materials Technology and Engineering, Chinese Academy of Sciences, Ningbo 315201, China
[b] Division of Functional Materials and Nano-devices, Chinese Academy of Sciences, Ningbo 315201, China

ABSTRACT

The scale behavior of Ti₂AlC coating at 750 °C in air and pure water vapor was investigated. A four-layered scale, a thick TiO₂ and Al₂O₃ mix oxide outer layer, followed by a thin α-(Al, Cr)₂O₃ sublayer, a thick Fe₂O₃ and TiO₂ mix oxide mid-layer and a thin Al₂O₃-rich oxide inner layer in sequence, developed on the Ti₂AlC coatings in air. Whereas internal oxidation occurred, no distinct oxide scale formed on the Ti₂AlC coating in the case of the oxidation in pure water vapor. The Ti₂AlC coating improved the oxidation resistance of 316LSS in air, especially in wet air.

© 2015 Elsevier B.V. All rights reserved.

1. Introduction

MAX phases are a group of nanolaminated materials, where M is an early transition metal, A an A-group element, and X either C or N [1]. This group of materials possess unique properties, such as high electrical and thermal conductivity, good machinability, excellent thermal shock resistance and damage tolerance, high elastic modules, high temperature strength, superior oxidation and corrosion resistances [2,3]. As one member of MAX phases, Ti₂AlC was attractive for high temperature structural applications. The high temperature oxidation behaviors of bulk Ti₂AlC have received great attention in the past decade [4–10]. At high temperature in dry air and water vapor a discontinuous TiO₂ outer layer and a continuous protective Al₂O₃-rich sub-layer form on the bulk Ti₂AlC, suggesting that Ti₂AlC exhibits excellent oxidation resistance. In contrast, Ti₃Al with higher Al content could not form a protective Al₂O₃ scale during oxidation [4–10].

Therefore, Ti₂AlC phase is expected to be one of the promising materials for high temperature corrosion protective coating applications. Ti₂AlC coating has been successfully prepared by numerous physical vapor deposition (PVD) processes [11–17] and high velocity oxy-fuel spray [18]. Thereafter, the oxidation behaviors of Ti₂AlC coating at high temperature in dry air were investigated [15–17]. The scale on the surface of Ti₂AlC coating by PVD consisted of a TiO₂-rich layer,

Al₂O₃-rich layer, and a TiO₂ + Al₂O₃ mixed layer in sequence at 800–900 °C in dry air. For TiAlC coating deposited by high velocity oxy-fuel spray technique there exist TiC and Ti₃AlC phases in the TiAlC which produce a discontinuous alumina, hence, decreasing its oxidation resistance [18]. Thus, the phase purity and microstructure have great influence on oxidation behavior of Ti₂AlC coating.

In addition, pure water vapor is a typical environmental condition in many energy related systems such as coal-fired power plant and nuclear power plant. Water vapor slightly accelerated the oxidation of Ti₂AlC due to the enhanced mass transportation process through the increased oxygen vacancy [8,9], while the influence of the presence of water vapor on the oxidation of Ti₂AlC coating is still unclear. Up to now, few works has focused on the oxidation behavior of Ti₂AlC coating at high temperature in pure water vapor.

In the present work, the oxidation behavior of the Ti₂AlC MAX phase coating, prepared on austenitic stainless steel by DC magnetron sputtering deposition and annealed, was investigated at 750 °C in dry air and pure water vapor, respectively. The scaling behavior was discussed based on the phase formation and microstructure evolution of the Ti₂AlC coating.

2. Experimental

Type 316 L austenitic stainless steels (316LSS) were used as the substrates alloy for the present work, with the nominal composition of 316LSS given as follows: Fe, bal; Cr, 16.0–18.0; Ni, 10.0–14.0; Mo, 2.0–3.0; C ≤ 0.03; Mn ≤ 2.00; Si ≤ 1.00; P ≤ 0.045; S ≤ 0.03. The steel plates were cut into specimens with the size of 15 mm × 10 mm × 2 mm,

* Corresponding authors at: Ningbo Institute of Materials Technology and Engineering, Chinese Academy of Sciences, Ningbo 315201, China. Tel.: +86 574 86685170; fax: +86 574 86685159.

E-mail addresses: kepl@nimte.ac.cn (P. Ke), aywang@nimte.ac.cn (A. Wang).

followed by grinding with 1000-grit SiC paper, and degreasing with acetone. The Ti–Al–C coating was deposited on the substrate by reactive DC magnetron sputtering with compound $Ti_{50}Al_{50}$ (at.%) target ($400 \times 100 \times 10$ mm^3) in Ar/CH$_4$ atmosphere with CH$_4$ as the reactive gas. The sputtering parameters were as follows: background vacuum 4.6×10^{-3} Pa; argon pressure 0.5 Pa; power 1.6 kW; room temperature; and sputtering time 10 h. Annealing treatment of the as-deposited coating was conducted at 800 °C in vacuum for 1 h to form the Ti$_2$AlC MAX phase. The details of the coating preparation can be found in our previous work [19].

The oxidation of the uncoated and coated 316LSS was isothermally conducted at 750 °C, which is a typical working temperature of next generation coal-fired power plant and nuclear power plant, in air and pure water vapor for 200 h, respectively. The air oxidation was carried out in static air. The pure water vapor oxidation was conducted in a high temperature tube furnace with a quartz tube as the reaction chamber. Ultrapure water with 5–7 mg/L dissolved oxygen content was pumped into the 400 °C preheated device to produce pure water vapor, which then flows into the reaction chamber. The pure water vapor flow rate was controlled to be 100–120 ml/s. The pressure of the pure water vapor was 0.1 MPa.

X-ray diffraction (XRD) using a Bruker D8 diffractometer with Cu K$_a$ radiation source was employed to characterize the phase formation. The surface and cross-sections of the samples were also examined by a FEI Inspect FSEM equipped with an Oxford energy dispersive X-ray (EDX) microanalysis.

3. Results and discussion

The Ti$_2$AlC MAX phase coating is mainly composed of Ti$_2$AlC phase with small amount of Ti$_3$AlC antiperovskite phase (Fig. 1a). Fig. 1b and c shows the surface morphology and cross-sectional morphologies of the Ti$_2$AlC coating. Due to the mismatch of thermal expansion coefficient between the Ti$_2$AlC phase and 316LSS, some through-cracks formed in the Ti$_2$AlC coatings. An Al-rich diffusion layer was also observed at the coating/substrate interface.

XRD analysis (Fig. 2a) reveals that 316LSS after oxidation at 750 °C in air for 200 h consisted of only Fe-rich (Cr,Fe)$_2$O$_3$. Fig. 2b and c shows the surface and cross-sectional morphologies of 316LSS after oxidation at 750 °C in air for 200 h. The steel oxidation in air formed a uniform scale mainly composed of Fe-rich oxides. Cross-sectional morphology showed that the thin Fe-rich scale was porous with poor adhesion to the substrate.

XRD analysis (Fig. 3a) indicates that the scale formed on the Ti$_2$AlC coating after oxidation at 750 °C in air for 200 h is mainly composed of α-(Al,Cr)$_2$O$_3$, θ-Al$_2$O$_3$ and rutile TiO$_2$. The surface morphology of the Ti$_2$AlC coating after oxidation at 750 °C in air for 200 h (Fig. 3b) showed clearly that the through-cracks present in the as-prepared coatings have been filled with Ti-rich oxides. However, no spallation was observed. The cross-sectional morphologies of Ti$_2$AlC coating after oxidation at 750 °C in air for 200 h showed that the scale exhibited a four-layered microstructure, a thick TiO$_2$ and Al$_2$O$_3$ mix oxide outer layer, followed by a thin α-(Al,Cr)$_2$O$_3$ sublayer, a thick Fe$_2$O$_3$ and TiO$_2$ mix oxide mid-layer and a thin Al$_2$O$_3$-rich oxide inner layer in sequence (Fig. 3c and d). No micropores or cracks were found at the Al$_2$O$_3$-rich oxide layer/substrate interface. Fig. 3e shows the corresponding EDX line scanned along the black line in Fig. 3d. EDX analysis indicated that the shape of the Cr curve agrees with that of Al curve. It is strongly confirmed that the sublayer is α-(Al,Cr)$_2$O$_3$. An Al-rich layer was detected at the coating/substrate interface, while an Al-depleted zone formed next to the coating/substrate interface. Beneath the Al-depleted zone, large amounts of Al-rich phase precipitation could be observed.
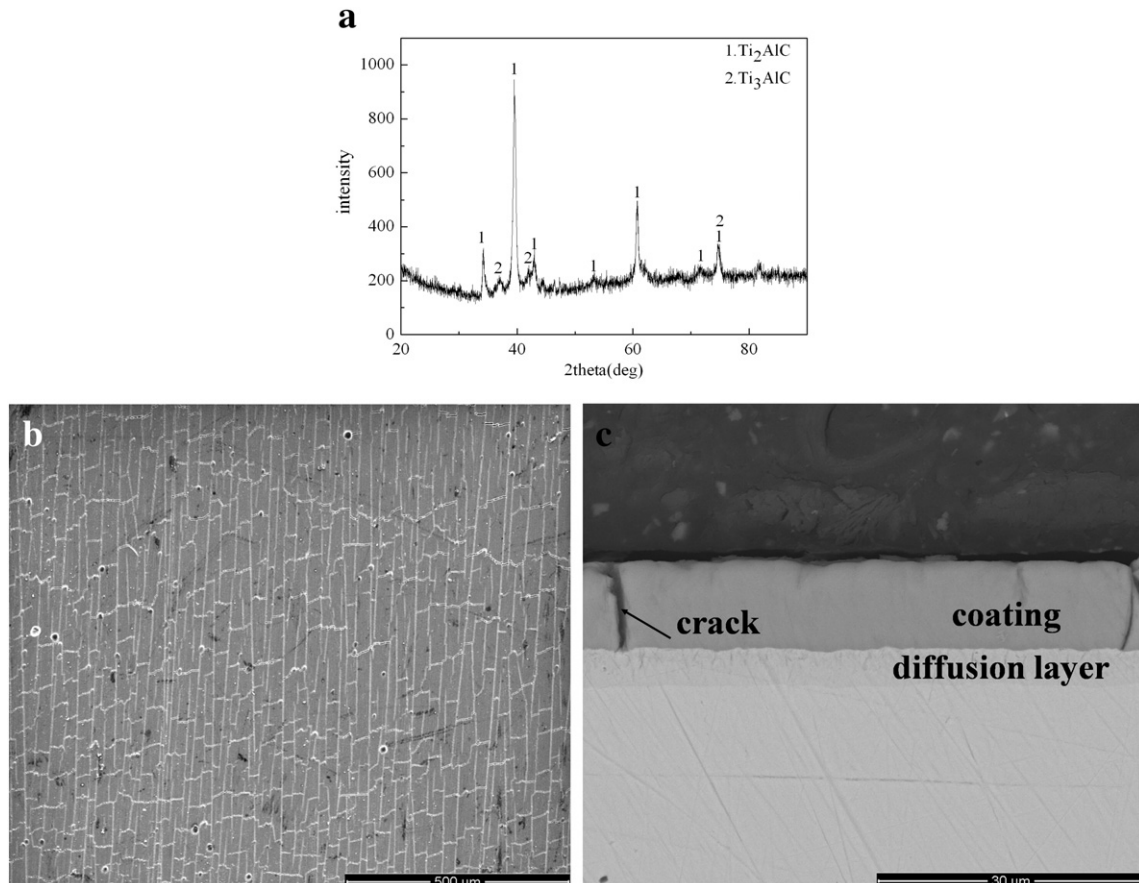

Fig. 1. XRD pattern (a), surface morphology (b) and cross-sectional morphologies (c) of the Ti$_2$AlC coating.
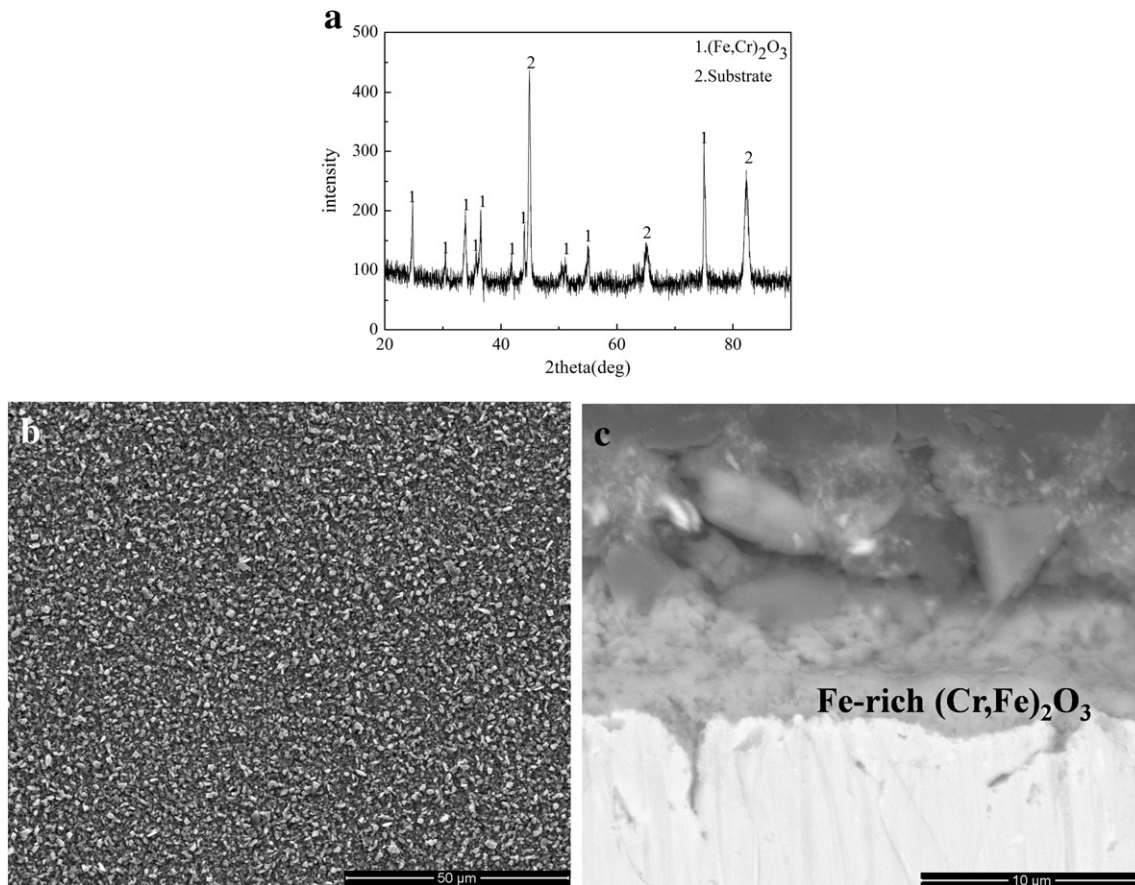
Fig. 2. XRD pattern (a), surface morphology (b) and cross-sectional morphologies (c) of 316LSS after oxidation at 750 °C in air for 200 h.

At the beginning of oxidation, both TiO_2 and Al_2O_3 could simultaneously form on the surface of the Ti_2AlC coating. The kinetics of the formation of TiO_2 is much faster than Al_2O_3 at low temperature and high oxygen partial pressure. Therefore the growth of TiO_2 layer is preferred. With the increasing of oxidation time, a continuous TiO_2 and Al_2O_3 mix oxide outer layer formed on the surface of the coating. As a result, the oxygen partial pressure at oxide layer/unreacted coating interface decreased. Once the oxygen partial pressure was lower than the TiO_2 equilibrium pressure, the TiO_2 would stop growing. Nevertheless, the oxygen equilibrium pressure of Al_2O_3 is lower than TiO_2. Meanwhile, Al atoms in the Ti_2AlC phase have a higher diffusion activity than that of Ti atoms [20,21], which is high enough to promote the oxidation of Al. In addition, the interdiffusion between the coating and substrate was unavoidable, and then Fe and Cr from substrate were diffused into the coating. As a result, a Cr solid solution α-$(Al,Cr)_2O_3$ sublayer formed at the TiO_2 and Al_2O_3 mix oxide layer/unreacted coating interface. Based on the above descriptions, the Ti_2AlC coating exhibits similar scaling behaviors with their bulk counterpart as reported by previous investigation [4,5]. Unfortunately, the Ti-rich oxides, which formed in the through-cracks presented in the as-prepared coatings, acted as a short-circuit diffusion path for the inward diffusion of oxygen. So the unreacted coating beneath the α-$(Al,Cr)_2O_3$ sublayer would oxidize and form a thick Fe_2O_3 and TiO_2 mix oxide mid layer. Furthermore, the lower oxygen partial pressure and the higher Al diffusion activity would promote the formation of a continuous Al_2O_3-rich oxide layer at the original coating/substrate interface. Finally, a four-layered microstructure scale, which possesses an excellent protectiveness to the substrate alloy, formed on the Ti_2AlC coating.

Water vapor is a typical environmental condition in many energy related systems, and usually water vapor will aggravate the oxidation behavior. XRD analysis (Fig. 4a) indicates that the scale formed on

316LSS after oxidation at 750 °C in pure water vapor for 200 h consisted of only Fe_2CrO_4. Fig. 4 shows the surface and cross-sectional morphologies of 316LSS after oxidation at 750 °C in pure water vapor for 200 h. In addition to a Fe_2CrO_4 scale, large amount of Fe_2O_3-rich nodules formed on 316LSS (Fig. 4b and c). 316LSS suffered from a non-uniform attack. In the fast oxidation area, 316LSS formed a thick scale consisted of an outer Fe-rich oxide layer and a Fe_2CrO_4 sublayer with a poor adhesion to the substrate, while in the other areas, only a Fe_2CrO_4 layer formed (Fig. 4d and e).

The breakaway oxidation of 316LSS clearly occurred as the generation of nodules after exposure to 750 °C pure water vapor 200 h. The scale formed in the incubation oxidation stage was mainly composed of thin protective Cr-rich oxide layer. The water vapor would significantly accelerate the oxidation of 316LSS. The vaporization of chromia scale from a protective Cr-rich oxide to a less protective $CrO_2(OH)_2$ has been proposed to explain the accelerated corrosion caused by water vapor [22–24]. As extending oxidation time, once the diffusion rate of Cr was insufficient to maintain an enough Cr concentration in the scale, the Cr-rich scale would lose re-healing ability. Then iron could diffuse easily outward to form non-protective nodules of Fe oxides. After that, the steel suffered from breakaway oxidation.

As for the Ti_2AlC coating after oxidation at 750 °C in pure water vapor for 200 h, the scale is mainly composed of rutile TiO_2, Al_2TiO_5, Ti_2AlC and Ti_3AlC (Fig. 5a). As seen in Fig. 5b, some oxide whiskers were detected at the through-cracks within the as-prepared coating, but the surface appearance of the as-prepared coating was retained to a certain extent. The coating after oxidation in pure water vapor was almost homogenous and no obvious oxide scale could be observed (Fig. 5c and d). In addition, a Fe-rich diffusion layer was presented at the original coating/substrate interface, with an Al-rich diffusion layer beneath it. The thickness of Al-rich diffusion layer was about double of
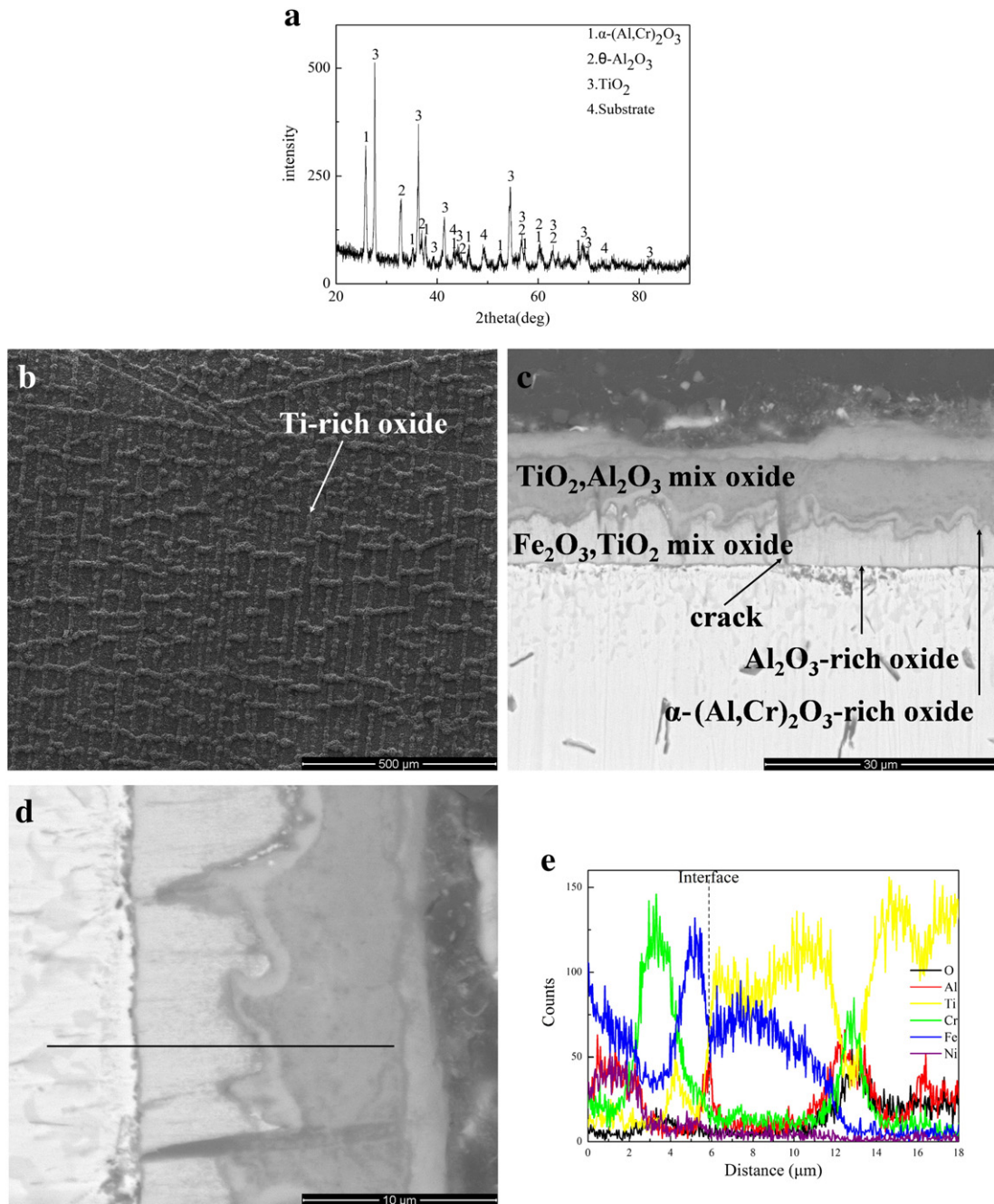
Fig. 3. XRD pattern (a), surface morphology (b), cross-sectional morphologies (c general view and d amplified view of c) of the Ti$_2$AlC coating after oxidation at 750 °C in air for 200 h, (e) the corresponding EDX line scanned along the black line in (d).

the as-prepared coating. And no obvious Al-rich phase precipitation was observed in the diffusion layer. EDX analysis (Fig. 5e) indicates that Fe was enriched near the coating/substrate interface. Al was depleted near the coating/substrate interface, but enriched beneath interface.

The scaling behavior of Ti$_2$AlC coating in pure water vapor was different from the scale behavior in air. The oxygen partial pressure is lower in pure water vapor than in air. It is generally believed that the low oxygen partial pressure will promote the formation of more thermodynamically stable Al$_2$O$_3$ oxide scale. However, in the present study, the unreacted Ti$_2$AlC phase still could be found and no distinct oxide scale formed on the Ti$_2$AlC coating after oxidation in pure water vapor. In contrast, the bulk Ti$_2$AlC exhibits a similar scaling behavior in wet air or pure water vapor as oxidation in dry air [8,9]. The generation of hydrogen from the reactions between Ti$_2$AlC and water vapor

promotes oxygen vacancy formation [8]. The increase in oxygen vacancy concentration facilitated the inward diffusion of oxygen, so the inward diffusion of the oxygen ions was higher than the outward diffusion of metal ions. In this circumstance, the activity of dissolved oxygen at the oxidation front was sufficiently high to maintain the internal oxidation. Additionally, due to the high diffusion activity of Al atoms in the Ti$_2$AlC phase than Ti atoms, the interdiffusion between the coating and the substrate, especially, the Al inward diffusion would further promote the degradation of the coating and not favor the formation of the Al$_2$O$_3$ oxide scale. Meanwhile, large amount Fe from the substrate alloy diffused into the coating. So the Al and Ti solute concentration of the coating was also lower than that required for the formation of a continuous scale. Then, the transition from internal to external oxidation could not occur, and no distinct oxide scale formed on the Ti$_2$AlC coating
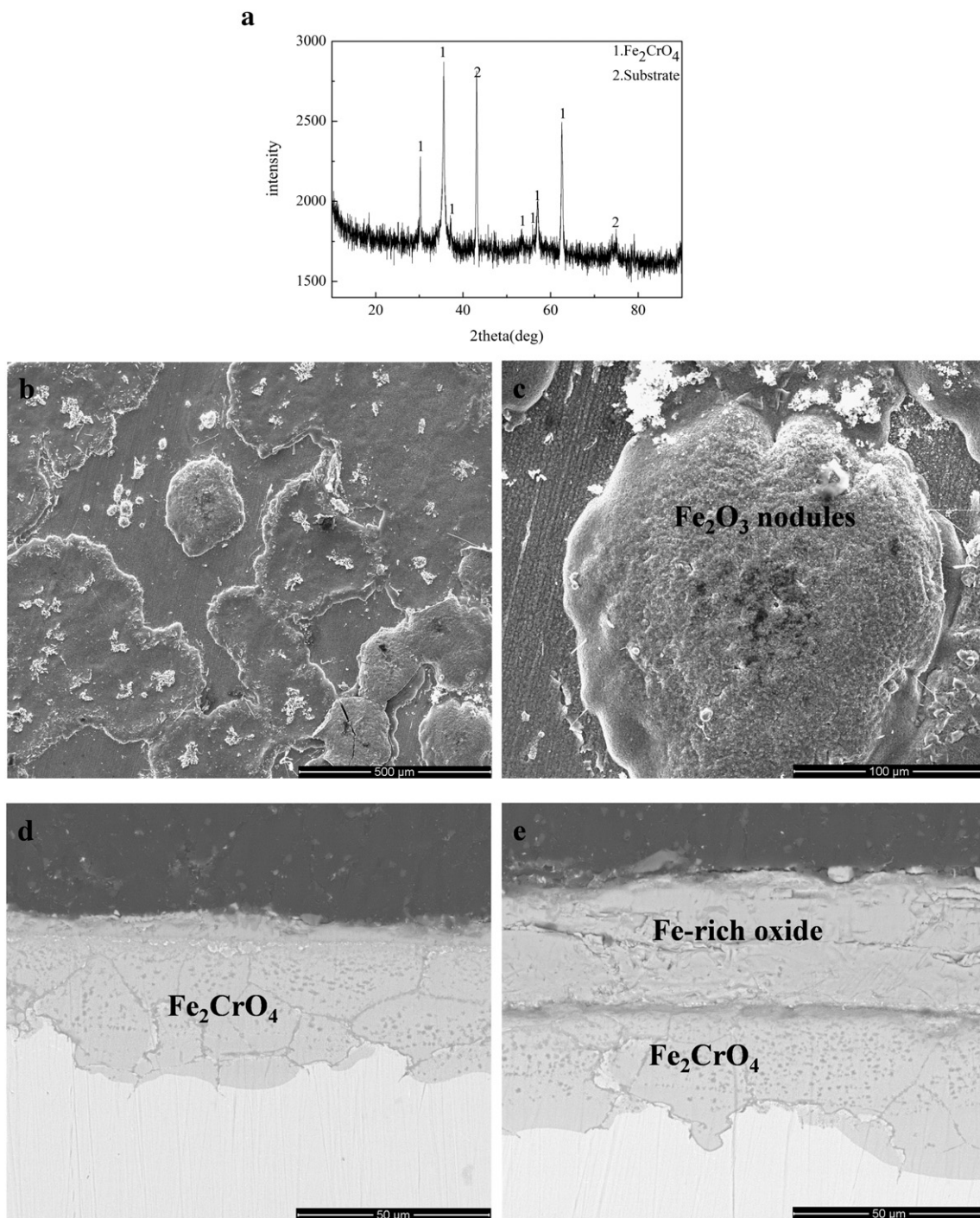
a

Fig. 4. XRD patterns (a), surface morphology (b), (c) and cross-sectional morphologies (d), (e) of 316LSS after oxidation at 750 °C in pure water vapor for 200 h.

after oxidation in pure water vapor. However, the Ti$_2$AlC coating could inhibit greatly the occurrence of breakaway oxidation of 316LSS substrate in pure water vapor.

Based on the above discussion, the schematic for the mechanism of the observed oxidation scaling which occurs at the interface between Ti$_2$AlC coatings and 316LSS substrate is presented in Fig. 6. A four-layered microstructure, a thick TiO$_2$ and Al$_2$O$_3$ mix oxide outer layer, followed by a thin α-(Al,Cr)$_2$O$_3$ sublayer, a thick Fe$_2$O$_3$ and TiO$_2$ mix oxide mid-layer and a thin Al$_2$O$_3$-rich oxide inner layer in sequence, formed on the Ti$_2$AlC coatings in air (Fig. 6a). Whereas internal oxidation occurred, no distinct oxide scale formed in the Ti$_2$AlC coating in

pure water vapor (Fig. 6b). In any case, the Ti$_2$AlC coating improves the oxidation resistance of 316LSS in both of air and pure water vapor.

4. Conclusion

The scaling behavior of Ti$_2$AlC MAX phase coating at 750 °C in air and pure water vapor was investigated. 316LSS could develop a protective oxide scale in air, while suffered from breakaway oxidation in pure water vapor. In contrast, the Ti$_2$AlC coatings could improve the oxidation resistance of 316LSS at certain content in both of air and pure water vapor. However, the oxidation resistance of the Ti$_2$AlC coating is
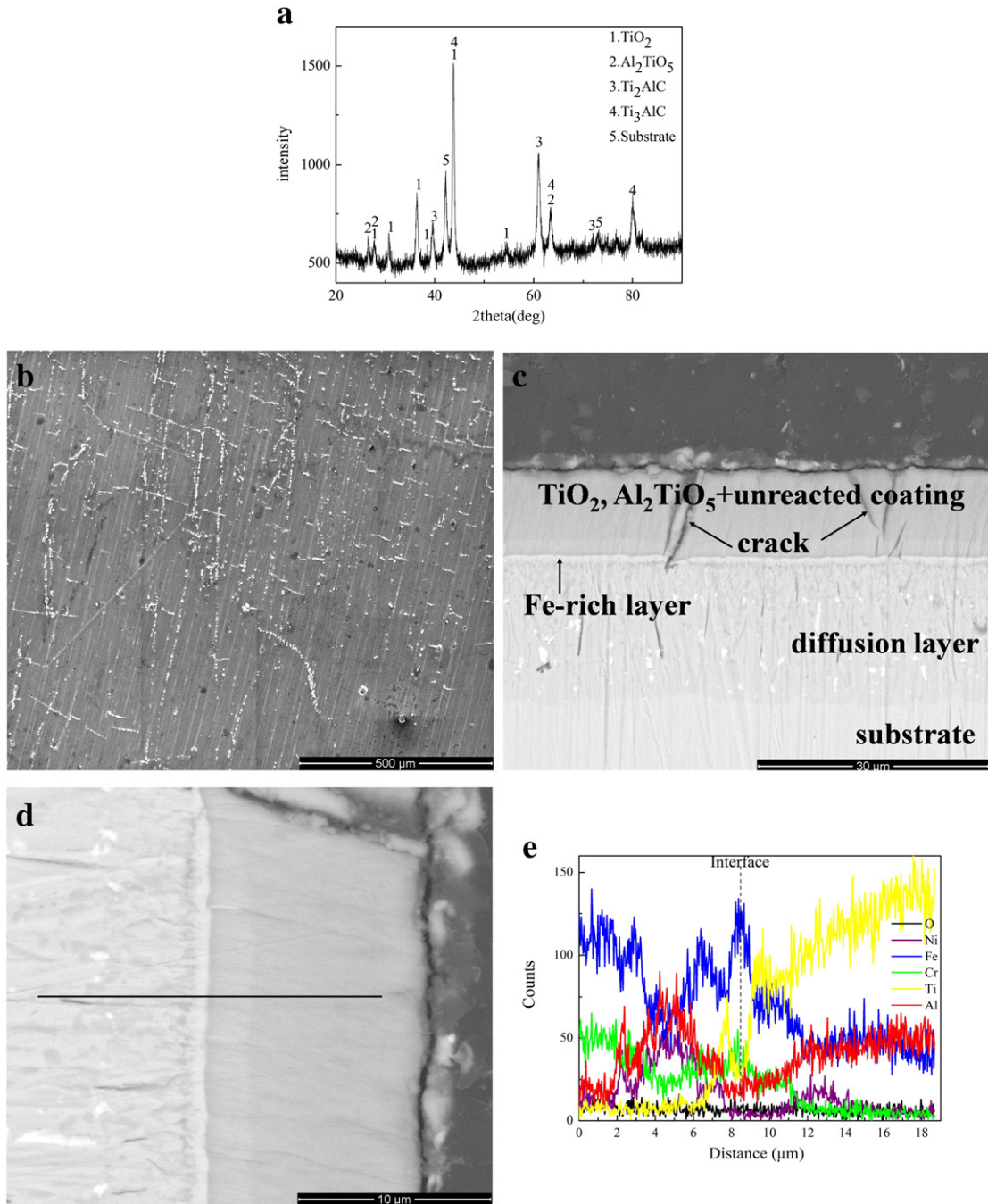
Fig. 5. XRD pattern (a), surface morphology (b) and cross-sectional morphologies (c general view and d amplified view of c) of the Ti$_2$AlC coating after oxidation at 750 °C in pure water vapor for 200 h, (e) the corresponding EDX line scanned along the black line in (d).

inferior to its bulk counterpart. The through-cracks presented in the as-prepared coating, which acted as a short-circuit diffusion path, the scaling ability of protective oxide could deteriorate. Due to the high diffusion activity of Al in the Ti$_2$AlC coating, the interdiffusion between the coating and the substrate would further accelerate the degradation of the Ti$_2$AlC coating. In the future, the main concern for the Ti$_2$AlC
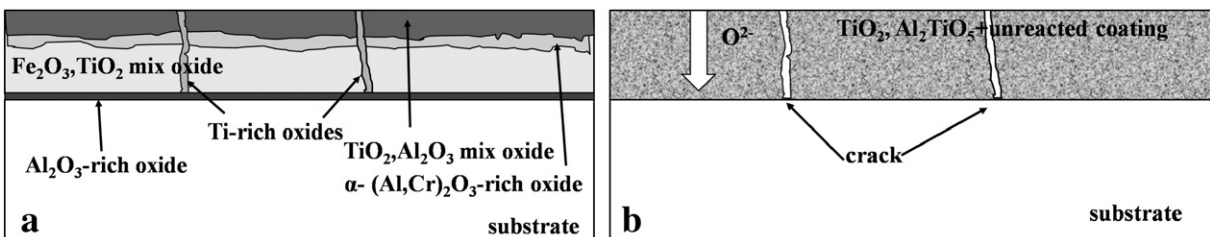

Fig. 6. Schematic of microstructural evolution of Ti$_2$AlC coating during oxidation (a) oxidation in high temperature dry air, (b) oxidation in water vapor.

coating is how to eliminate through-cracks in the as-prepared coating. Meanwhile, an appropriate diffusion barrier layer should be application at the Ti$_2$AlC coating/substrate interface.

References

[1] M.W. Barsoum, Prog. Solid State Chem. 28 (2000) 201–281.
[2] P. Eklund, M. Beckers, U. Jansson, H. Högberg, L. Hultman, Thin Solid Films 518 (2010) 1851–1878.
[3] Z.M. Sun, Int. Mater. Rev. 56 (2011) 143–166.
[4] X.H. Wang, Y.C. Zhou, Oxid. Met. 59 (2003) 303–320.
[5] X.H. Wang, Y.C. Zhou, J. Mater. Res. 17 (2002) 2974–2981.
[6] B. Cui, D.D. Jayaseelan, W.E. Lee, Acta Mater. 59 (2011) 4116–4125.
[7] H.J. Yang, Y.T. Pei, J.C. Rao, J.Th.M. De Hosson, S.B. Li, G.M. Song, Scr. Mater. 65 (2011) 135–138.
[8] Z.J. Lin, M.S. Li, J.Y. Wang, Y.C. Zhou, Scr. Mater. 58 (2008) 29–32.
[9] S. Basu, N. Obando, A. Gowdy, I. Karaman, M. Radovic, J. Electrochem. Soc. 159 (2012) C90–C96.
[10] G.P. Bei, B.J. Pedimonte, T. Fey, P. Greil, J. Am. Ceram. Soc. 96 (2013) 1359–1362.
[11] J. Frodelius, P. Eklund, M. Beckers, P.O.Å. Persson, H. Högberg, L. Hultman, Thin Solid Films 518 (2010) 1621–1626.
[12] W. Garkas, C. Leyens, A. Flores Renteria, Adv. Mater. Res. 89–91 (2010) 208–213.
[13] A. Abdulkadhim, T. Takahashi, D. Music, F. Munnik, J.M. Schneider, Acta Mater. 59 (2011) 6168–6175.
[14] M.C. Guenette, M.D. Tucker, M. Ionescu, M.M.M. Bilek, D.R. McKenzie, Thin Solid Films 519 (2010) 766–769.
[15] Q.M. Wang, W. Garkas, A. Flores Renteria, C. Leyens, H.W. Lee, K.H. Kim, Corros. Sci. 53 (2011) 2948–2955.
[16] M. Fröhlich, in: W.M. Kriven, Y. Zhou, M. Radovic, S. Mathur, T. Ohji (Eds.), Strategic Materials and Computational Design: Ceramic Engineering and Science Proceedings, vol. 31, John Wiley & Sons, Inc, Hoboken, NJ, USA 2010, pp. 161–169.
[17] J. Frodelius, J. Lu, J. Jensen, D. Paul, L. Hultman, P. Eklund, J. Eur. Ceram. Soc. 33 (2013) 375–382.
[18] M. Sonestedt, J. Frodelius, M. Sundberg, L. Hultman, K. Stiller, Corros. Sci. 52 (2010) 3955–3961.
[19] Z.J. Feng, P.L. Ke, A.Y. Wang, J. Mater. Sci. Technol. (2015) (accepted for publication).
[20] N.K. Othman, N. Othman, J. Zhang, D.J. Young, Corros. Sci. 51 (2009) 3039–3049.
[21] D.J. Young, High Temperature Oxidation and Corrosion of Metals, Elsevier, Oxford, 2008. 455–495.
[22] J.Y. Wang, Y.C. Zhou, T. Liao, J. Zhang, Z.J. Lin, Scr. Mater. 58 (2008) 227–230.
[23] B. Liu, J.Y. Wang, J. Zhang, J.M. Wang, F.Z. Li, Y.C. Zhou, Appl. Phys. Lett. 94 (2009) 181906.
[24] H. Asteman, K. Segerdahl, J.E. Svensson, L.G. Johansson, Mater. Sci. Forum 369–372 (2001) 277–286.